

Optimized offset Modulation Technique For Three-phase DC-AC Boost- Converter

S. pouresmaeil¹, b.skandari²

¹Malayer university, Electrical Faculty, Hamadan,iran

¹Email : pouresmaeil.ieee@gmail.com

² PhD candidate in K. N. Toosi University of Technology,

²Email : eskandari@ieee.org

M. Tavakoli Bina

Professor of K. N. Toosi University of Technology

Tehran,iran

Email : tavakoly@kntu.ac.ir

Abstract— This paper introduces an efficient modulation technique for three-phase DC-AC boost converter. various modulation scheme have already been developed for conventional three-phased boost converter such as sinusoidal pwm (spwm) and space vector modulation (svm).there are two main considerations in designing power electronic converter;small-size simple topology and applicable control algorithm. This paper starts with an ideal differential boost-inverter, suggesting a simple formulation of pulse widths for generation of sinusoidal waveform. Despite some improvements on the waveforms, still the output voltage is distorted. It is notable that even PI-controllers followed by various modulating techniques still lead to distorted output voltage because of the non-linear structure of conver.further,to overcome the state issue an optimized offset modulation technique is defined for conventional six-pulse two-level three-phase boost-converter. Furthermore, practical verification are taken place on implemented 1 kVA boost-converters in order to confirm the proposed technique as well as theoretical analysis and simulations. Experiments and simulations both verify the suggested optimized modulation technique.

Keywords–Modulation,Three-phase boost – converter,Optimized offset,Differential connection

I. INTRODUCTION

In recent years, serious concerns have been raised over the fossil fuel electricity generation, because it pollutes our environment and depletes the energy supply. As a result, alternative energy sources, such as solar energy and fuel cells, have gained great attention because they are friendly to the environment and flexible for installation. However, these types of sources produce dc power while the present power grid accepts ac power; therefore, grid-connected inverters are necessary for dc–ac conversion. The inverters are desired to have high power quality, high efficiency, high reliability,lowcost, and simple circuitry. As far as the alternative source is concerned, the photovoltaic (PV) module or fuel cell stack usually supplies a dc voltage lower than the peak grid voltage, and their output voltage varies in a wide range according to various operation conditions [1],[2]. Thus, the needed converter has to boost the generated voltage by the PV and then convert it to AC (alternatively the AC output could be boosted). These two tasks (booster and DC-AC

conversion) are controlled independently; each creates its own power losses [3],[4]. Surveying literatures shows some suggestions on combining these two independent controlled tasks, proposing topologies that perform simultaneously both the DC voltage level and DC/AC conversion [5-8]. The question, however, is that how the switching pulses should be arranged to generate a sinusoidal output voltage. Various modulating techniques were suggested for these combined converters in order to generate sinusoidal waveforms; for example, using adaptive control based on the state space equations [8-12]. While these complicated control techniques disregard the differential boost structure, this research intentionally concentrates on the differential structure in order to improve the performance in general [13-16].This paper starts with an ideal differential boost-inverter, suggesting a simple formulation of pulse widths for generation of sinusoidal waveform. Despite some improvements on the waveforms, still the output voltage is distorted. It is noticeable that even PI-controllers followed by various modulating techniques still lead to distorted output voltage due to the non-linear structure of converter. Further, to overcome the stated issue, an optimized offset modulation technique is defined for conventional six-pulse two-level three-phase boost-converter.. Finally, in order to verify the proposed modulation techniques as well as theoretical analysis and simulations, practical verifications are performed on implemented 1 kVA boost-converter. In brief, analysis and experiments show that the proposed modulation technique is mathematically simple to implement, lowers the DC-link current oscillations of the boost-type converter, high efficiency and low THD.

II. THREE-PHASE BOOST INVERTER

A. Topology

This converter is consists of three dc-dc boost converters shown in Fig.1. Therefore, it's expected from each one of the three DC-DC boost-converters to produce a sinusoidal voltage along with some DC offset. Analysis of the three-phase boost-converter as three separated DC-DC boost type converter is the main theoretical background of this paper. However, producing a pure sinusoidal voltage is hard to achieve because the gain of a real DC-DC boost-converter severely depends on the load current, especially at higher gains. In other words,

production of a time-dependent gain (sinusoidal waveform) will include large distortions. Various modulating techniques were suggested for three-phase boost-converter in order to generate sinusoidal waveforms; for example, using adaptive control based on the state space equations [5-8]. While these complicated control techniques disregard the differential boost structure, this research intentionally concentrates on the differential structure in order to improve the performance in general.

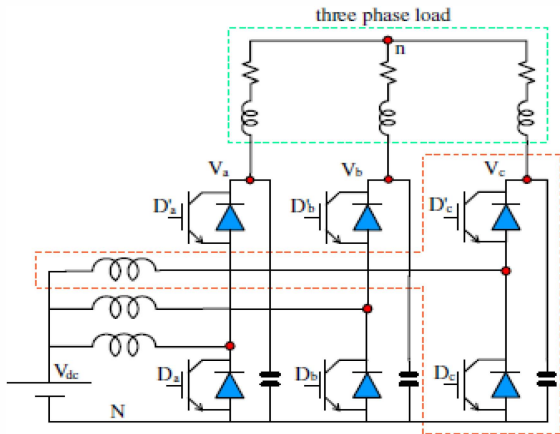


Fig. 1: Three-phase DC-AC boost-converter.

B. Suggesting Differential pulse-widthmodulation technique for three-phase boost converter

Assume the principal goal is to build up three phase-to-phase independent sinusoidal voltages at the load terminal of Fig. 1. It is obvious that the gain of the boost converter starts from one when all the controllable switches are always off. Thus, each phase of the boost-inverter in Fig. 1 has a DC offset with respect to the negative pole of the battery. Figure 2 illustrated the amount of this offset, i.e.

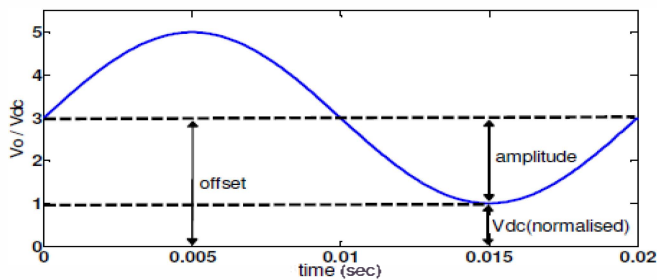


Fig2. Normalized desire output, capacitor voltage, of one leg of the boost-inverter.

1)formulation: Based on the gain of an ideal DC–DC boost converter; assume these voltages are modulated with the following duty cycles as bellow:

$$\begin{cases} V_{av}(t) = \frac{V_{dc}}{1 - D_a} = A \sin(\omega t) + A + V_{dc} \\ V_{bv}(t) = \frac{V_{dc}}{1 - D_b} = A \sin(\omega t + 120^\circ) + A + V_{dc} \\ V_{cv}(t) = \frac{V_{dc}}{1 - D_c} = A \sin(\omega t + 240^\circ) + A + V_{dc} \\ A > V_{dc} \end{cases} \quad (1)$$

where D_a , D_b and D_c are duty cycles for the three legs, V_{dc} is the DC offset of each boost-inverters (that is the amplitude of the input source), and A is the amplitude of the sinusoidal voltages. Note that the boost-inverter voltages have always the same sign as V_{dc} ; hence, A has to be added to keep this necessary condition. By differentiating any two boost voltages in (1), the line voltages of the load are obtained as follows:

$$\begin{cases} V_{ab} = V_a - V_b = \sqrt{3}A \sin(\omega t - 30^\circ) \\ V_{bc} = V_b - V_c = \frac{V_{dc}}{1 - D_a} = \sqrt{3}A \sin(\omega t + 90^\circ) \\ V_{ca} = V_c - V_a = \frac{V_{dc}}{1 - D_c} = \sqrt{3}A \sin(\omega t - 150^\circ) \end{cases} \quad (2)$$

Therefore the phase-to-neutral voltages at the load are:

$$\begin{cases} V_{an} = \frac{V_{dc}}{1 - D_a} = A \sin(\omega t) \\ V_{bn} = \frac{V_{dc}}{1 - D_b} = A \sin(\omega t + 120^\circ) \\ V_{cn} = \frac{V_{dc}}{1 - D_c} = A \sin(\omega t + 120^\circ) \end{cases} \quad (3)$$

These ideal outcomes can be achieved by calculating the three-phase duty cycles using (1):

$$\begin{cases} D_a = 1 - \frac{V_{dc}}{A \sin(\omega t) + A + V_{dc}} \\ D_b = 1 - \frac{V_{dc}}{A \sin(\omega t + 120^\circ) + A + V_{dc}} \\ D_c = 1 - \frac{V_{dc}}{A \sin(\omega t + 240^\circ) + A + V_{dc}} \end{cases} \quad (4)$$

2)Simulation of PWM: In order to verify (4) in a three-phase boost-inverter, a series of simulations have been performed using SIMULINK. Figure.3 represent the block diagram of new proposed PWM. As an example, let us assume $A = 4 \times \sqrt{24} / 3$ and $V_{dc} = 24$ V; then, duty cycles for a whole power cycle (20ms) is worked out according to (4). Figure.4 illustrates simulated duty cycles (D) produced by (4).

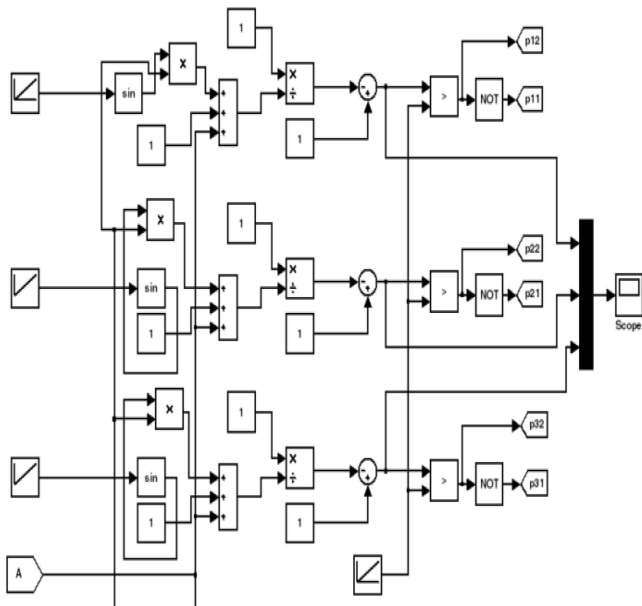


Fig.3. block diagram for generation PWM

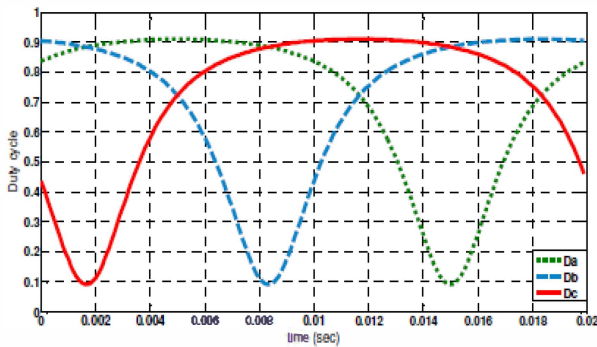
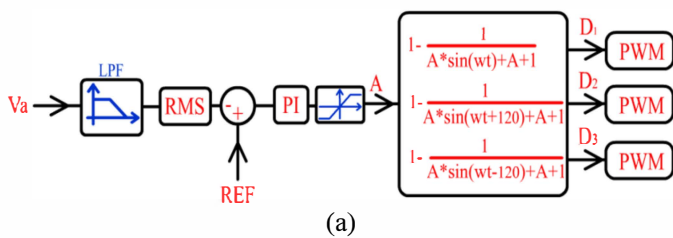


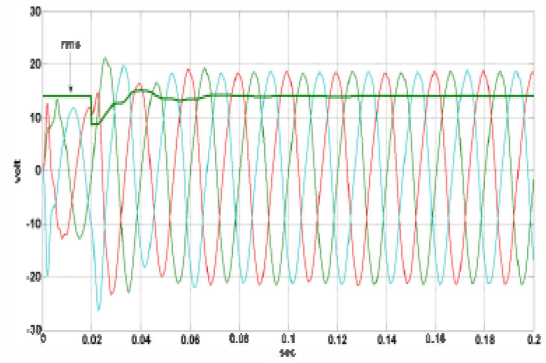
Fig.4. simulated duty cycles by(4)

C. Applying the PI-controller to the boost-inverter

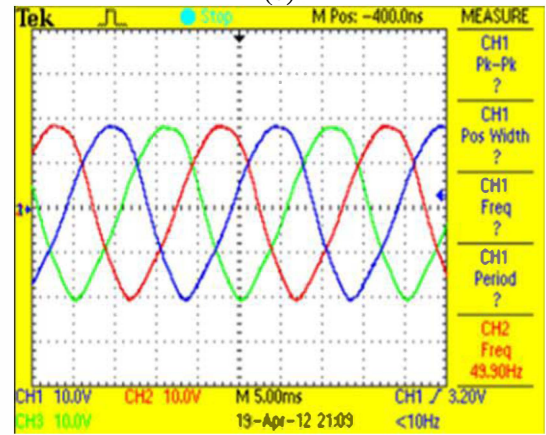
In practice, one may think of a PI-controller as a regulator of the output voltage of a converter at a certain reference RMS value. This closed-loop PI-controller was also applied to the boost-inverter, both in simulation and practice, where Fig. 8 (a) shows the applied PI loop. Figure 8 (b) shows the simulation results. It can be seen that while the output voltage



(a)



(b)



(c)

Fig. 5. Application of the PI controller to regulate the output voltage of boost-inverter, (a) control diagram, (b) the simulated RMS voltage has been traced by a PI-loop, and (c) experimental recorded voltages while both distortion and unbalance peak magnitude still remain in place.

RMS value is regulated at 15 V, both distortion and unbalance peak magnitude still remain in place at large. To confirm simulations, the implemented boost-inverter was also programmed; the PI-controller was uploaded on the DSP in order to regulate the output voltage. Fig. 5 (c) confirms the simulations.

D. Specifications of the implemented boost-converter

A 1 kVA boost-converter was implemented according to Fig. 1. This is used as a practical prototype for evaluating the performance of the suggested modulation technique. The power circuit includes two series 12V, 55 Ah batteries as the input DC voltage V_{dc} , three 200 μ H inductors (10A), three 250 μ F capacitors (100V) and six IGBTs (BUP314D). Drivers of the switches are fed through four isolated DC supplies, where the coupler TLP250 interfaces the microprocessor and the power circuit. A three-phase laboratory L-C set as the output filter and a 2kW, 380V induction motor were used as the load. The microprocessor is the EZDSP TMS320F28335 that regulates pulse widths for the six switches using code composer studio (CCSTUDIO). Figure 4 shows the implemented three-phase boost-converter described above.

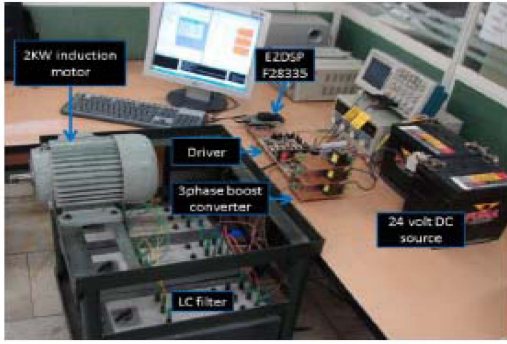
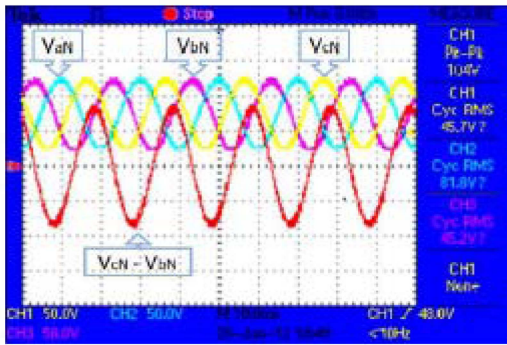


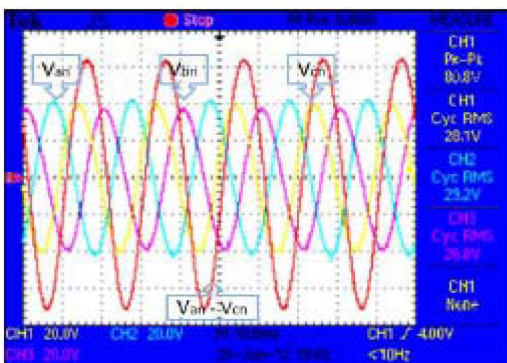
Fig.6: The implemented three-phase 1 kVA boost-converter for studying the suggested modulation techniques

E. Description and analysis of the experimental results

Typical calculated duty cycles shown in Fig. 4 were programmed with the CCSTUDIO on the EZDSPF28335 to drive the six switches of the boost-converter. Three phase-to-neutral voltages (V_{an} , V_{bn} and V_{cn}) and three phase-to-negative pole of the DC source (V_{aN} , V_{bN} and V_{cN}) were recorded through a serial port as shown in Fig. 5. Studying Fig. 7(a) shows clearly the amount of added DC offset to all three phases. Also, the difference between two outputs of individual DC-DC boost-converters ($V_{cN} - V_{bN}$) is shown in Fig.7 (b), where the presence of L-C filters remove the high frequency ripples of load voltages. The significant point is that the experiments agree well with simulations.



(a)



(b)

Fig. 7: Experimental results, (a) three phase-to-negative voltages, and (b) three phase-to-neutral voltages

F. Offs et optimization

Practical work verifies that the proposed fixed offset modulator is capable of producing three-phase sinusoidal voltages with bigger amplitude compared to the source voltage (V_{dc}). Interestingly, reduction of this fixed offset will pave the way for efficient generation of sinusoidal output voltages because of lower duty cycles. Further, it comes to the mind investigating the possibility of varying the DC offset instead of working with a fixed offset. Hence, let the total offset be variable, named as $X(t)$. Then, relationships (1) can be rearranged as follows:

$$\begin{cases}
 V_{aN}(t) = \frac{V_{dc}}{1-D_a} = A \sin(\omega t) + A + X(t) \\
 V_{bN}(t) = \frac{V_{dc}}{1-D_b} = A \sin(\omega t + 120^\circ) + A + X(t) \\
 V_{cN}(t) = \frac{V_{dc}}{1-D_c} = A \sin(\omega t + 240^\circ) + A + X(t) \\
 V_{aN}(t) + V_{bN}(t) + V_{cN}(t) = 3X(t)
 \end{cases} \quad (5)$$

Thus, the aim is to minimize the variable DC offset $X(t)$ or $V_{aN} + V_{bN} + V_{cN}$. In fact, an optimization problem is defined to achieve a time-dependent minimized offset as below:

Minimize: $V_{aN}(t) + V_{bN}(t) + V_{cN}(t)$
 Subjected to:

$$\begin{cases}
 V_{cN}(t) - V_{bN}(t) = \frac{V_{dc}}{1-D_c} = \sqrt{3}A \sin(\omega t - 30^\circ) \\
 V_{bN}(t) - V_{aN}(t) = \frac{V_{dc}}{1-D_a} = \sqrt{3}A \sin(\omega t - 90^\circ) \\
 V_{aN}(t) \geq 1, V_{bN}(t) \geq 1, V_{cN}(t) \geq 1 \\
 A \geq 1
 \end{cases} \quad (6)$$

The normalized value of $\sqrt{3}A$ is equal to 4 for the given example of Fig. 4. Solving the above optimization problem needs to be repeated for several points during one period of power frequency f_p . If f_s is the switching frequency, then the number of points is equal to f_s/f_p . Throughout this paper f_p and f_s are 50Hz and 10 kHz, respectively; therefore, the number of samples will be 200 points. The optimization problem (6) was repeated to solve for all 200 points as shown in Fig. 8 (a). Replacing the obtained outcomes of the optimization problem in (5) with $X(t)$, the new three-phase duty cycles will be concluded.

The results of the optimization problem for each phase demonstrate interesting regularly repeated shapes. It can be seen from Fig. 8 (a) that the variable DC offset is divided into four certain patterns; combining DC offset numbered as 1 with that of 4 results in a unified mirrored of part 2. Part 3 introduces no DC offset. Figure 8(b) demonstrates three duty cycles under variable DC offset. In order to verify the performance of the proposed optimization method, these optimized calculated duty cycles are applied to the implemented boostconverter. Experimental results are shown in Figs. 8(c) – (d), confirming the proposed analysis and simulations.

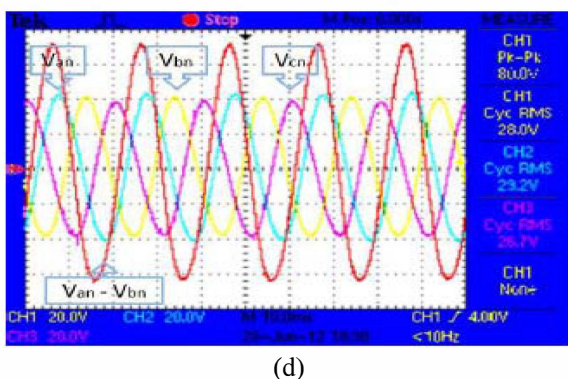
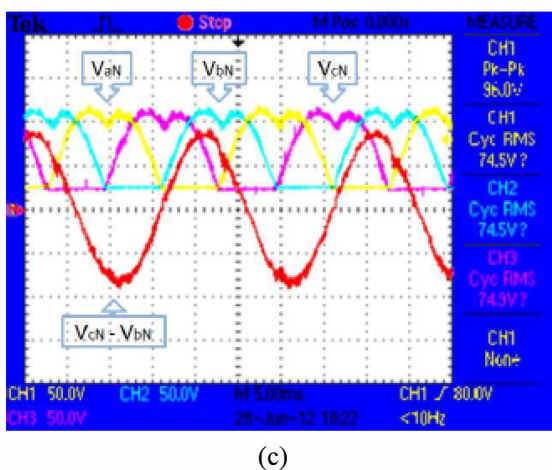
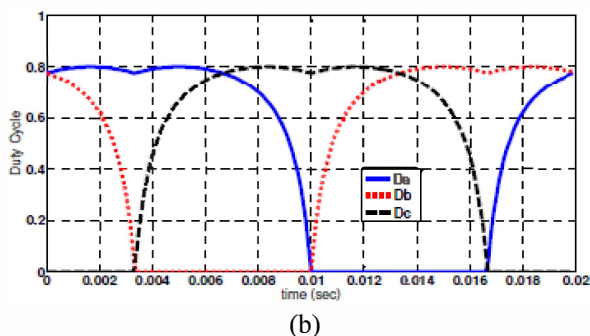
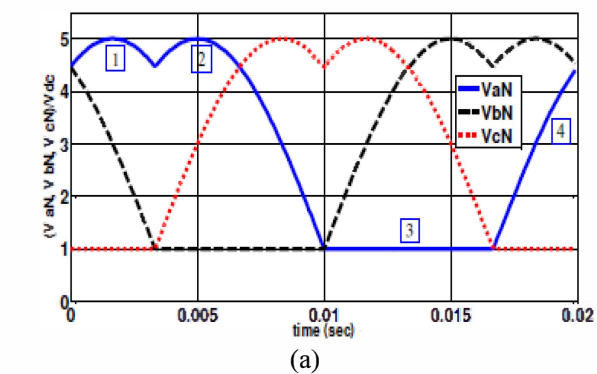
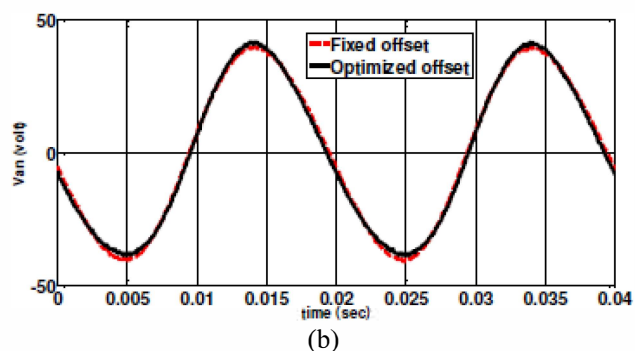
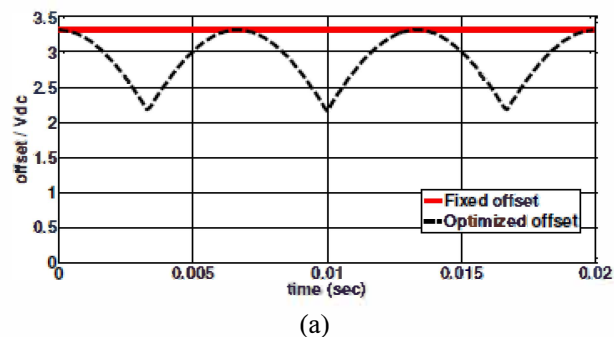
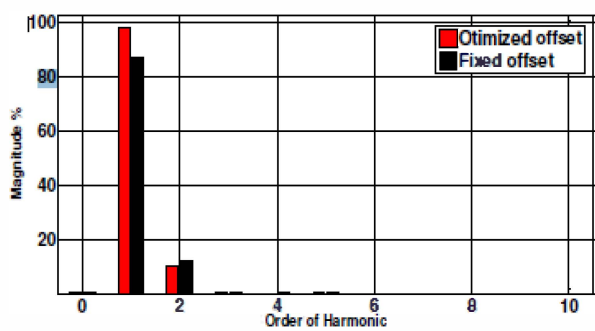


Fig. 8: Optimization results, (a) three phase-to-negative voltages, (b) produced duty cycles by (5), experimental results (minimized offset for boost-converter), (c) three phase-to-negative voltages, and (d) three phase-to-neutral voltages.

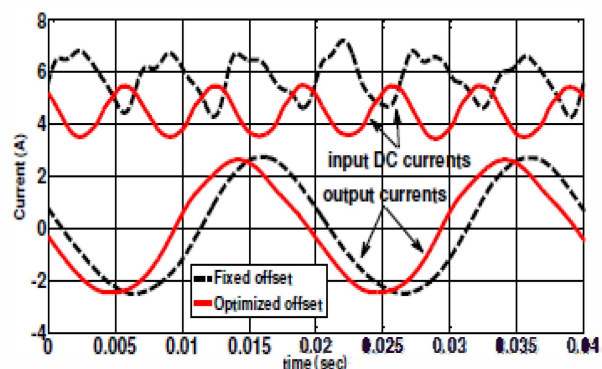
E. Analytical discussions

An analytic comparison can be studied based on experiments on both the fixed and the optimized offset techniques to find out their performances in practice. To establish a valid comparison, identical amplitudes for line voltages are considered at the load terminals for both techniques (4×24 volt). The boost-inverter was uploaded by the two modulating techniques, and their corresponding outcomes were recorded for further discussions. Figure. 9 (a) shows the DC offset ($V_{An} + V_{bN} + V_{cN} / 3$) obtained by the two suggested modulation techniques. While the produced offset by the optimized technique is smaller than the fixed offset throughout a power period (20ms), removing part of the needed active power due to the harmonics from the source. It should be noted that the lower the total DC offset in (2) would result in lower turn on times of the switches. Further, generated fundamental voltages are introduced in Fig. 9 (b), where their THD were also calculated by obtaining the spectra of output voltages as demonstrated in Fig. 9(c). These pictures state that the optimized offset provides slightly bigger fundamental compared to the fixed offset. Also, the THD for the fixed and the optimized techniques are 6% and 4%, respectively. Moreover, both the input and output currents for the two techniques can be compared in Fig. 9 (d). It is clear that the DC source current is considerably lower for the optimized offset under the same loading conditions in comparison with the fixed offset. At the same time, the phase of the output current is much closer to the fundamental output voltage for the optimized offset. Additionally, Figs. 10 (a)–(b) present the optimized offset (V_{An}), both simulations and experiments that strongly confirms theoretical discussions and analysis.



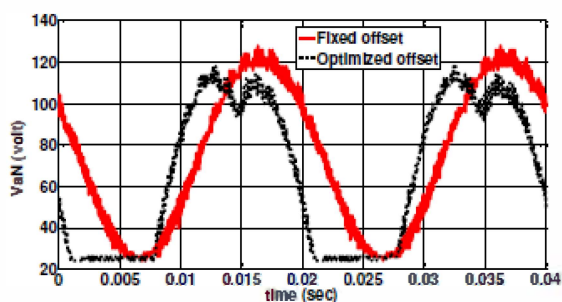


(c)

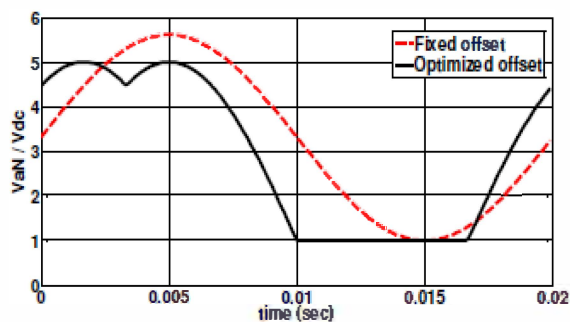


(d)

Fig. 9: A comparison between (a) the amount of fixed and optimized offset, and (b) output voltages (V_{aN}), (c) spectrum of output voltages, and (d) input and output currents of both techniques.



(a)



(b)

Fig. 10: Output voltages (V_{aN}) of both techniques (a) experiments, and (b) simulations

CONCLUSION :

This paper analyzes the structures of three-phase differential boost-type converter based on three separate DC-DC boost-converters. It is shown that the DC offset plays an important role in the modulation techniques. An efficient modulation technique, the optimized offset modulation, is proposed that is applicable to three-phase converters. Major contributions of the proposed modulating strategy includes lower calculations and lower DC link current oscillations in boost-type converters compared to the other strategies. Two experimental test sets were designed to evaluate the proposed modulation techniques for boost -converter. Experimental results of the boost-converter indicate considerable impacts on the improved modulation as well as current reduction of the DC source.

REFERENCES

- [1] Shen, J. M., Jou, H. L.: 'Transformer-less three-port grid-connected power converter for distribution power generation system with dual renewable energy sources', *IET Power Electron.*, 2012, 5, (4), pp. 501-509
- [2] Yufei, Z., Wenxin, H.: 'Single-Stage Boost Inverter With Coupled Inductor', *IEEE Trans. Power Electron.*, 2012, 27, (4), pp. 1885-1893
- [3] Gautam, D. S., Bhat, A. K. S.: 'A Comparison of Soft-Switched DC-to-DC Converters for Electrolyzer Application', *IEEE Trans. Power Electron.*, 2013, 28, (1), pp. 54 - 63
- [4] R. W. Erickson, —Fundamentals of Power Electronics, □ *New York: Chapman and Hall*, pp. 40-50, May 1997.
- [5] Carlo Cecati, Senior Member, IEEE, Antonio Dell'Aquila, Member, IEEE, and Marco Liserre, Member, IEEE, —A Novel Three-Phase Single-Stage Distributed Power Inverter, □ *IEEE Trans. Power Electron.*, vol. 19, pp. 1226 - 1233, no. 5, Sep. 2004.
- [6] Gu, B., Dominic, J., Lai, J., Liu, Z. Z. C.: 'High Boost Ratio Hybrid Transformer DC-DC Converter for Photovoltaic Module Applications', *IEEE Trans. Power Electron.*, 2013, 28, (4), pp. 2048-2058
- [7] Valderrama-Blavi, H., Bosque, J. M., Guinjoan, F., and Martinez-Salamero, L. M.: 'Power Adaptor Device for Domestic DC Micro grids Based on Commercial MPPT Inverters', *IEEE Trans. Ind. Electron.*, 2013, 60, (3), pp. 1191-1203
- [8] Chu, G., Chi, K., Tse, R., Chung Wong, S., Tan, S.C.: 'A unified approach for the derivation of robust control for boost PFC converters', *IEEE Trans. Power Electron.*, 2009, 24, (11), pp. 2531-2544
- [9] Zhu, M., Yu, K., and Luo, F. L.: 'Switched Inductor Z-Source Inverter', *IEEE Trans. Power Electron.*, 2010, 25, (8), pp. 2150-2158.
- [10] Rezvanyardom, M., Adib, E., Farzanehfard, H.: 'New interleaved zero-current switching pulse-width modulation boost converter with one auxiliary switch', *IET Power electronic.*, 2011, 4, (9), pp. 979-983
- [11] Chen, Y., and Smedley, K.: 'Three-Phase Boost-Type Grid-Connected Inverter', *IEEE Trans. Power Electron.*, 2008, 23, (5), pp. 2301-2309
- [12] Hausmann, R., and Barbi, I.: 'Three-Phase DC-AC Converter Using Four-State Switching Cell', *IEEE Trans. Power Electron.*, 2011, 26, (7), pp. 1857-1867
- [13] Lai, Y. S., Lin, Y. K., and Chen, C. W.: 'New Hybrid Pulsewidth Modulation Technique to Reduce Current Distortion and Extend Current Reconstruction Range for a Three-Phase Inverter Using Only DC-link Sensor', *IEEE Trans. Power Electron.*, 2013, 28, (3), pp. 1331-1337
- [14] Dupczak, B. S., Perin, A. J., and Heldwein, M. L.: 'Space Vector Modulation Strategy Applied to Interphase Transformers-Based Five-Level Current Source Inverters', *IEEE Trans. Power Electron.*, 2012, 27, (6), pp. 2740-2751
- [15] Govindaraju, C., Baskaran, K.: 'Efficient Sequential Switching Hybrid-Modulation Techniques for Cascaded Multilevel Inverters', *IEEE Trans. Power Electron.*, 2011, 26, (3), pp. 1639-1648
- [16] Zhang, D., Wang, F., El-Barbari, S., Sabate, J. A., and Boroyevich, D.: 'Improved Asymmetric Space Vector Modulation for Voltage Source Converters with Low Carrier Ratio', *IEEE Trans. Power Electron.*, 2012, 27, (3), pp. 1130-1140